Optimal Design and Comparison of Synchronous Machines with Inner and Outer Reluctance Rotors and PM or DC Stator Combined Excitation

Oluwaseun A. Badewa, Ali Mohammadi, Donovin D. Lewis, and Dan M. Ionel
SPARK Laboratory, Stanley and Karen Pigman College of Engineering, University of Kentucky, Lexington, KY, USA
o.badewa@uky.edu, alimohammadi@uky.edu, donovin.lewis@uky.edu, dan.ionel@ieee.org

***Abstract*—This paper presents an optimal design and comparative analysis for a toroidally wound reluctance rotor synchronous machine with either PM or DC excitation in the stator. The prototype of the PM version is experimentally evaluated, and its results are used to validate the model of the DC version as they share the same topology. The stator DC-excited synchronous (SDCES) motor is optimized at different outer diameters using large-scale multi-objective differential evolution (DE) and comparatively analyzed at power ratings typical for electric traction and propulsion applications. Its performance at reduced temperatures shows increased efficiency and goodness due to reduced losses, and its ability to employ modularity ensures high-reliability and fault-tolerant operation, which is critical for electric propulsion and traction applications.**

***Index Terms*—Electric traction, propulsion, synchronous motor, spoke-type PM, magnet-free, castellated rotor, fault-tolerant, cryogenic operation, finite element analysis.**

I. Introduction

The application of electric motors in traction and propulsion has grown in recent years, driven by the conflicting goals of achieving higher power density and efficiency while reducing costs [1]. Permanent magnet (PM) motors continue to be an industry favorite due to their ability to deliver substantial power output within a compact and lightweight design, making them particularly advantageous when space and weight constraints are critical factors [2]–[5].

Recently, specialty topologies have been proposed to employ non-rare earth PMs, such as ferrites and FeN, achieving a power density similar to that of rare earth PMs. One such example is the spoke-type PM arrangement for flux intensification [6]–[8]. Completely magnet-free motors using DC excitation instead of PMs, as described in [9], [10], are also a topic of interest due to their benefits of reduced cost, potential fault tolerance, and improved controllability.

The machine topology explored in this paper is a toroidally wound synchronous machine with all active components located in the stator and a reluctance rotor. Variants of the base design can employ non-rare earth PMs and DC toroidal or wave windings for stator excitation, taking advantage of the spoke-type arrangement and flux intensification. Previous work has identified several advantages including high power density, the elimination of demagnetization concerns, and wide torque-speed operational range. Additionally, these machines offer the potential for a high slot fill factor with hairpin wound Litz wire and reduced losses [11], [12].

The castellated reluctance rotor in these designs allows for easy construction and high-speed operation. The active stator having either PM or DC excitation, allows for the implementation of advanced stator-only cooling. This cooling method allows for possibility of operation at reduced or cryogenic temperatures, offering benefits such as reduced copper losses and increased PM remanence, ultimately improving efficiency and power density. These advantages are particularly desirable for electric traction and propulsion applications [13], [14].

Given the critical nature of electric propulsion, there is a continuous search for fault-tolerant motors and drive systems. This is pursued through ongoing reliability and fault diagnostic studies Examples of fault-tolerant operation implementations in the literature include the use of redundancy in modular multilevel converters (MMCs) as described in [15], multi-stage machine concept in [16], and machine learning for motor control in [17], [18].

This paper compares synchronous machines with reluctance rotors and toroidally wound stators, employing either PMs or DC excitation. A multi-objective optimization is formulated and applied to PM and DC stator-excited outer-rotor machines using experimentally validated FEA models in ANSYS Maxwell. Additionally, the fault-tolerant and cryogenic operation of the DC-excited motor are also studied to investigate the potential benefits of the proposed topology [19].

II. Motor topologies, Computational Models, and Reference Prototype

The PM stator-excited motor features an active outer stator with circumferentially magnetized PMs, concentrated toroidal coils that form 3-phase AC windings, and a castellated consequent pole rotor, as shown in Fig. 1a. A PM stator-excited motor design variant is an outer rotor configuration that enhances flux intensification by using longer PMs in the inner stator. The stator DC-excited synchronous (SDCES) motor variant, shown in Fig. 2, has a similar configuration, with the key difference being that DC excitation coils replace the PMs.

Both motor designs have toroidal coils, which are naturally concentrated and offer benefits such as improved copper slot fill and reduced losses due to shortened end turns. These machines use consequent-pole castellated rotors with no active

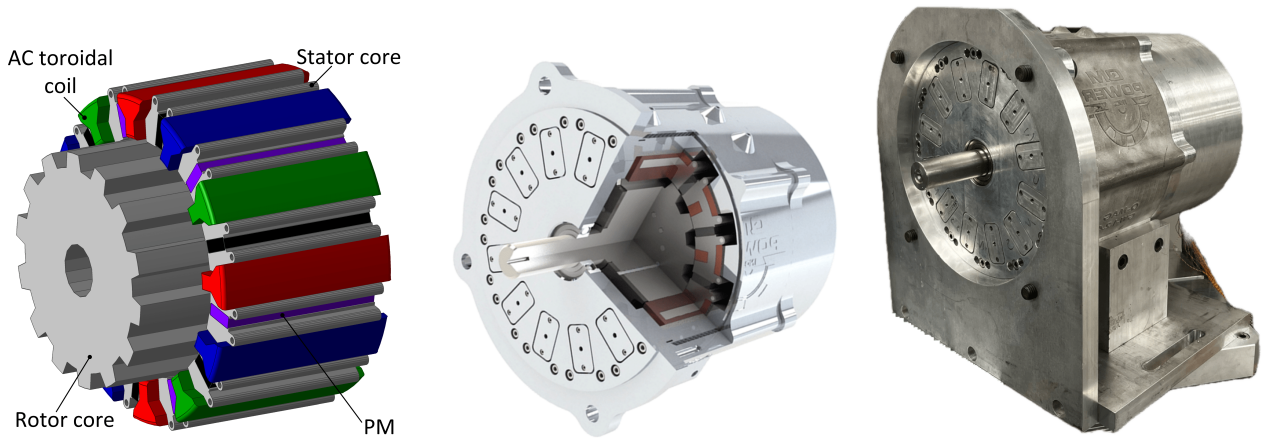

(a) (b) (c)

Fig. 1. The investigated PM stator-excited motor topology as a (a) solid model for 3D FEA with labelled component parts, (b) 3D CAD model, and (c) constructed prototype.

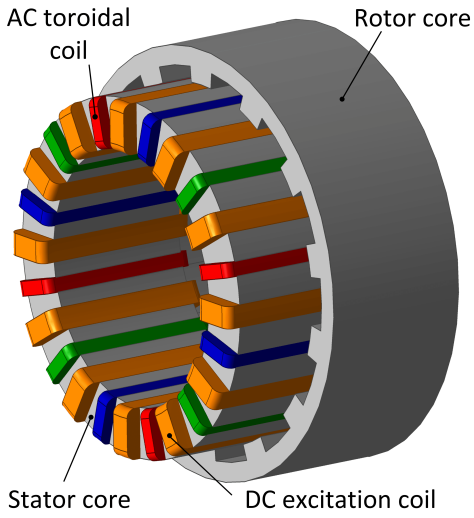

Fig. 2. A solid model for 3D FEA of the SDCES motor with toroidal AC and DC coils, and a reluctance outer rotor.

components, the number of rotor protrusions corresponds to the principal pole pair number, for example, 14 rotor protrusions result in a 28-pole machine. The absence of active elements in the rotor enables high-speed operations and the application of advanced cooling techniques [11], [13], [20]. The operational principles of the PM and DC-excited machines are explored in greater detail in [12], [21].

In the PM stator-excited motor topology, particularly in an outer rotor configuration, the flux concentration ratio is a function of the PM height, h_{PM}, along the radius, as detailed in [21]. Additionally, the motor torque is directly influenced by the airgap diameter, D_g, as elaborated in Lehr *et al.* [22]. These findings led to the development of an outer rotor design variant that is magnet-free and has a larger rotor diameter for higher power density.

The DC-excitation variant shown in Fig. 2 leverages the principles of flux intensification while addressing concerns related to PM sourcing, prices, and demagnetization. The outer rotor SDCES motor has the advantage of a larger airgap diameter for high power density, PM-free operation, adaptability to integrated advanced cooling, and toroidal coils in rectangular slots suitable for the latest hairpin winding technology. Additionally, its segmented stator allows for fault-tolerant operation, making it a competitive candidate for electric traction and propulsion applications [12], [16].

While both PM and DC-excited motor variants offer several benefits, concerns include the cost of rare-earth PMs and additional electronics and control infrastructure. These challenges can be mitigated by using ferrites or innovative PMs, such as Niron, especially in an outer rotor configuration for the PM stator-excited motor, and by employing a simple fixed uncontrolled DC excitation supply [6], [21], [23].

Both configurations also employ open slots, which lead to eddy currents and supplementary losses due to relatively large magnetic field variations [24], [25]. Reduction in the slot opening and the use of Litz wire are typical mitigation techniques for optimal torque output and loss reduction [26]. The associated high common mode (CM) current and electromagnetic interference (EMI) issues for toroidal windings can also be managed through design strategies, as detailed in [27].

Following the analysis and modeling of the PM stator inner rotor design, a prototype has been modeled and constructed, as shown in Figs.1b and 1c. The results of the locked rotor test and static torque constant measurements are shown in Figs. 3a and 3b, respectively, demonstrating good agreement between the FEA and experimental results for the prototype, thereby offering validation. The FEA model of the prototype was then used as a foundational model for subsequent 2D FEA models, including the SDCES.

III. Multi-objective Design Optimization

Parametric models of the outer rotor SDCES motor with 14 rotor protrusions (14-P) were optimized with outer rotor diameters of 255mm for electric traction and 500mm for

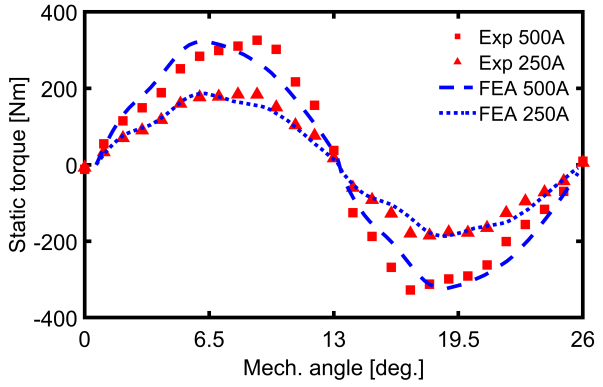

(a)

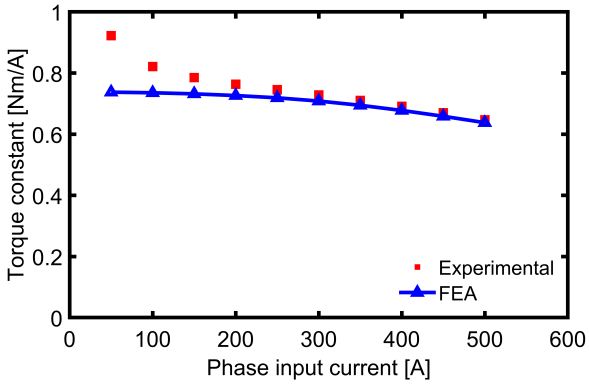

(b)

Fig. 3. Comparison of experimental and FEA results for the PM stator-excited prototype showing good correlation for (a) the locked rotor test at currents of 250A and 500A, and (b) the static torque constant with increasing phase currents.

electric propulsion within a fixed volume. Multi-objective optimization employing differential evolution (DE) and FEA was carried out with three concurrent objectives.

The three optimization objectives F1, F2, and F3 are to *maximize* electromagnetic torque, T_e, maximize the power factor, pf, and *minimize* the motor loss, P_{loss}, respectively at a speed of 3,000rpm, typical for traction and electric aircraft applications. The motor loss, P_{loss}, is considered the sum of constant core losses (P_{Fe}), and variable copper losses (P_{Cu}). Optimal ranges were set for the independent geometrical variables based on parametric studies to yield mechanically stable designs within a wide optimization space [2].

The optimization results for the 255mm OD designs are shown in Fig. 4 with the optimal Pareto designs highlighted in red, and with the selected "best" design marked with a black star. This design is scaled by stack length to achieve the desired power rating. The cross-sectional views for the selected "best" designs for the 255mm and 500mm ODs, along with their flux lines and density plots, are shown in Fig. 5.

IV. Results and Discussion including Cooling and Fault Tolerant Operation

The comparative analysis between the PM prototype design and the optimal design of the SDCES is documented in Table I. Performance indexes such as machine goodness, specific torque, specific power, and power density are evaluated at power ratings typical for light and heavy-duty electric vehicle (EV) and electric propulsion applications. An optimal design of the SDCES at an outer diameter of 255mm is compared with the tested, scaled, and simulated versions of the PM prototype. In line with expectations, the PM stator-excited motor exhibits

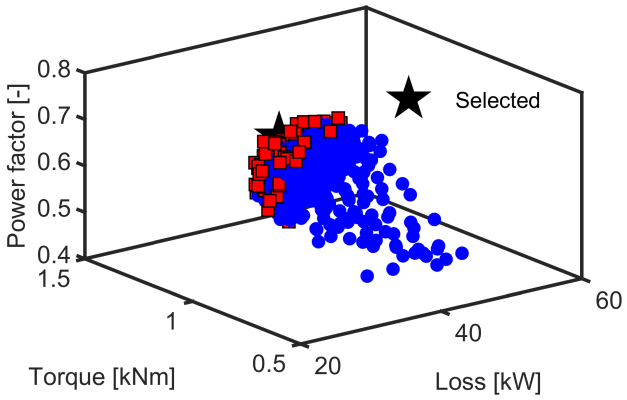

(a)

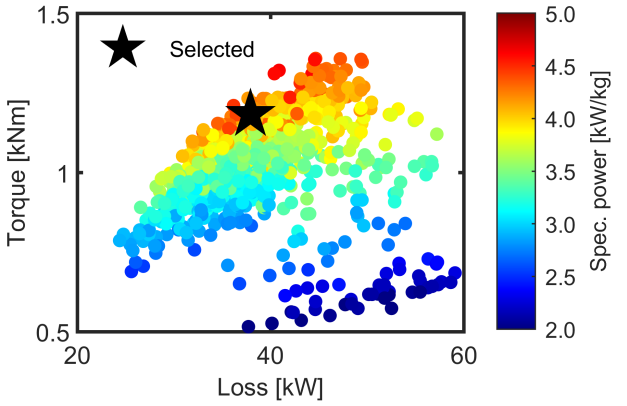

(b)

Fig. 4. Multi-objective optimization results for 255mm OD SDCES with (a) Pareto front designs in red and selected design marked with a black star, and (b) a projection illustrating the high specific power.

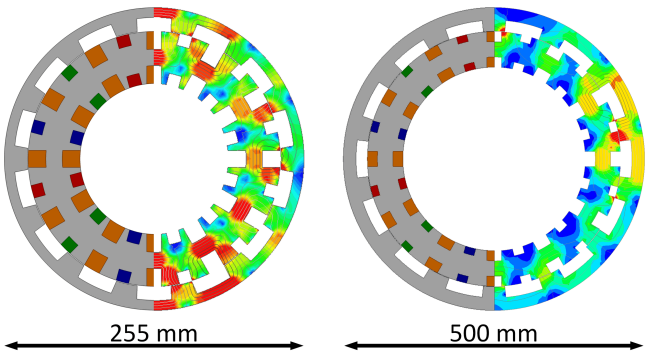

Fig. 5. Cross-sectional views of optimal selected designs for SDCES with 255mm and 500mm ODs, showing flux lines and densities at peak loading.

Table I
CHARACTERISTICS OF PM STATOR-EXCITED PROTOTYPE AND SDCES DESIGN OPERATING AT 3,000RPM AND ROOM TEMPERATURE

	PM stator-excited motor prototype			SDCES
Configuration		Inner rotor		Outer rotor
Status	Tested	Scaled	Simulated	Simulated
Rated power [kW]	100	150	250	250
Torque [Nm]	319	479	798	794
Goodness [Nm/sqrt(W)]	3.0	3.6	7.7	4.8
Specific torque [Nm/kg]	7.6	7.6	8.6	13.1
Specific power [kW/kg]	2.4	2.4	2.7	4.1
Power density [kW/L]	15.4	15.4	19.3	18.4

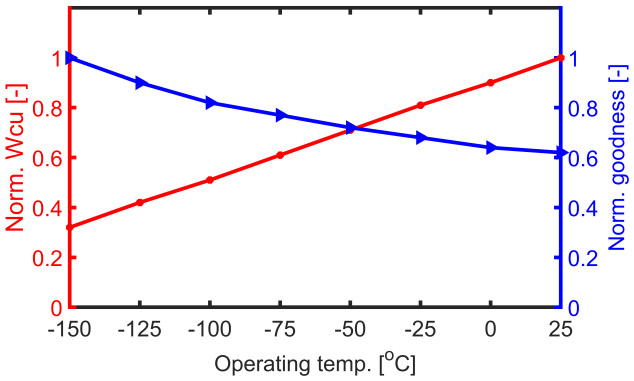

Fig. 6. Parametric analysis on the effect of cooling on total copper losses Wcu and goodness in a 1.5MW SDCES motor showing the possibility for reduced losses and improved machine goodness at lower temperatures.

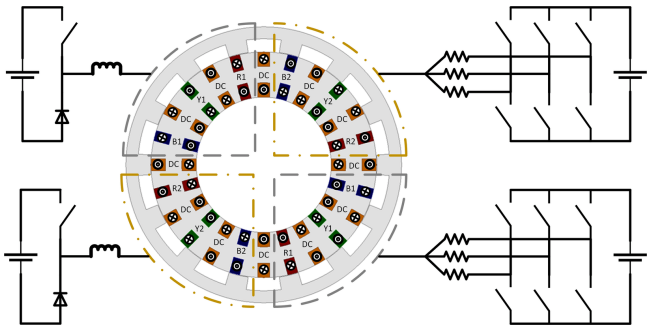

Fig. 7. Example SDCES motor employing two independently powered diagonal stator halves, represented by the dashed and dotted dashed lines fault-tolerant operation.

higher machine goodness than the SDCES due to its use of PMs as the excitation source. However, it has lower specific power and torque because of its demagnetization constraints. For a larger outer diameter of 500mm, the SDCES can achieve a simulated specific power greater than 5.4kW/kg and power density greater than 15.7kW/L for a power rating of 250 kW. At a power rating of 1.5 MW, it can achieve a specific power of 6.2 kW/kg and a power density of 23.7 kW/L. This indicates improved competitive performance at larger diameters.

The application of advanced cooling, expected to be typical for electric propulsion, is assumed when evaluating the performance of the SDCES motor at 1.5MW operating at 3,000rpm. Total copper loss (W_{cu}) and associated machine goodness which is the ratio of torque to the squared route of losses, were evaluated in simulations with varying temperatures, as

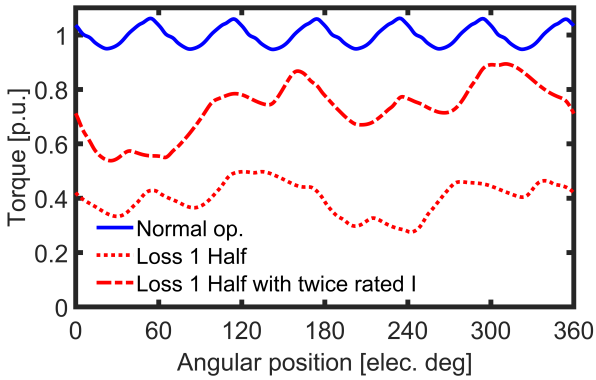

Fig. 8. Simulated normal and possible fault operating conditions for a dual sector 1.5MW SDCES motor showing operation with the loss of one diagonal sector and its energization with twice the rated current.

shown in Fig. 6. At an operating temperature of -150°C, copper losses can be reduced by about 65%, and the overall machine goodness can increase by 40%. The cost and size implications of using such a cooling system must be considered to ensure that high specific power and power density are maintained.

Furthermore, the SDCES allows for the implementation of stator segmentation to enhance fault tolerance. This design enables the machine to operate with two electrically separated stator halves, each powered by a different inverter, as illustrated in Fig. Fig. 7 [28].

Performance under normal and fault conditions, such as the loss of an entire segment (resulting in complete 3-phase AC and DC excitation loss in one segment), is summarized in Fig. 8. Even with the loss of one diagonal half of the SDCES machine, fed by one converter, it can still operate at approximately half of its full capacity.

The associated power electronics and machine windings can be designed so that in the event of the loss of one entire diagonal half, the functional half can be powered with double the rated AC and DC currents, enabling the machine to operate at about 75% capacity with the potential for increased torque ripple, as shown in Fig. 8. Therefore, in terms of fault tolerance—particularly crucial in propulsion applications—the SDCES demonstrates the capability for segmentation, providing robust fault-tolerant operation and enhanced reliability.

V. CONCLUSION

In this paper, two machines were proposed, modeled, and optimized, both employing all active excitation in the stator: one with permanent magnets and one with DC windings. The inner rotor machine with PMs was experimentally prototyped and tested to validate the effectiveness of 2D ANSYS Maxwell FEA models used for motor analysis and optimization. The outer rotor machine with stator DC excitation represents a variant of the same topology, which eliminates the possibility of demagnetization.

The proposed DC-excited motor was optimized for outer diameters of 255 mm and 500 mm, which are typical for electric traction and propulsion applications. It was comparatively analyzed with the prototyped PM version, with results indicating

that the PM version exhibits better machine performance and higher efficiency. The DC-excited version, on the other hand, excels in specific power, especially at larger outer diameters. Further studies have demonstrated that the SDCES motor can achieve enhanced performance at lower temperatures and enable high-efficiency, high-reliability, fault-tolerant operation through machine segmentation. This capability is crucial for electric propulsion and traction applications.

ACKNOWLEDGMENT

This research was funded by the National Aeronautics and Space Administration (NASA) University Leadership Initiative (ULI) #80NSSC22M0068. The material presented in this paper does not necessarily reflect the views of NASA. The support of QM Power, Inc., ANSYS, Inc., and the University of Kentucky the L. Stanley Pigman Chair in Power Endowment is gratefully acknowledged.

REFERENCES

[1] B. Fahimi, L. H. Lewis, J. M. Miller, S. D. Pekarek, I. Boldea, B. Ozpineci, K. Hameyer, S. Schulz, A. Ghaderi, M. Popescu, B. Lehman, and D. D. Patel, "Automotive electric propulsion systems: A technology outlook," *IEEE Transactions on Transportation Electrification*, pp. 1–1, 2023.

[2] M. Rosu, P. Zhou, D. Lin, D. M. Ionel, M. Popescu, F. Blaabjerg, V. Rallabandi, and D. Staton, *Multiphysics simulation by design for electrical machines, power electronics and drives*. John Wiley & Sons, 2017.

[3] E. Sayed, S. M. Castano, J. W. Jiang, J. Liang, G. Pietrini, M. H. Bakr, A. Emadi, and B. Bilgin, "Design of multilayer concentric ferrite-magnet machines for a traction application," *IEEE Transactions on Transportation Electrification*, vol. 7, no. 3, pp. 1548–1560, 2021.

[4] W. Feng, K. Chen, J. Paddock, T. Jahns, and B. Sarlioglu, "Design and comparison of surface inset permanent magnet machine and surface permanent magnet machine without heavy rare earth magnets for traction applications," in *2023 IEEE Energy Conversion Congress and Exposition (ECCE)*, 2023, pp. 4022–4029.

[5] G. Volpe, F. Marignetti, S. Roggia, M. Popescu, and J. Goss, "Performance validation of a PM spoke machine for motorsport application including 3Dleakage effects," in *2018 IEEE Transportation Electrification Conference and Expo (ITEC)*, 2018, pp. 394–399.

[6] P. C.-K. Luk, H. A. Abdulrahem, and B. Xia, "Low-cost high-performance ferrite permanent magnet machines in EV applications: A comprehensive review," *eTransportation*, vol. 6, p. 100080, 2020.

[7] M. R. Hoyt, G. I. Falcon, C. J. Pearce, R. E. Delaney, T. E. Stevens, E. M. Johnson, T. M. Szenderski, N. R. Sorenson, S. F. Fultz-Waters, M. A. Rodriguez, L. J. Whalen, and T. C. Monson, "Fabrication and characterization of net-shaped iron nitride-amine-epoxy soft magnetic composites," *Frontiers in Materials*, vol. 10, 2023.

[8] D. Ionel, D. Jackson, G. Starr, and A. Turner, "Permanent magnet brushless motors for industrial variable speed drives," in *2002 International Conference on Power Electronics, Machines and Drives (Conf. Publ. No. 487)*, 2002, pp. 650–654.

[9] I. P. Wiltuschnig, A. F. F. Filho, B. H. B. Boff, and P. R. Eckert, "Design and analysis of a novel axial variable-flux reluctance machine with DC-Excited field and modular double rotor," *IEEE Transactions on Energy Conversion*, pp. 1–10, 2024.

[10] L. Boscaglia, H. S. N. Sugumar, N. Sharma, and Y. Liu, "Design and verification of an electrically excited synchronous machine rotor with direct oil cooling for truck applications," *IEEE Transactions on Transportation Electrification*, pp. 1–1, 2024.

[11] C. S. Goli, M. G. Kesgin, P. Han, D. M. Ionel, S. Essakiappan, J. Gafford, and M. D. Manjrekar, "Analysis and design of an electric machine employing a special stator with phase winding modules and PMs and a reluctance rotor," *IEEE Access*, vol. 12, pp. 9621–9631, 2024.

[12] O. A. Badewa, A. Mohammadi, D. M. Ionel, S. Essakiappan, and M. Manjrekar, "Electric vehicle traction motor with a reluctance outer rotor and a modular stator with AC concentrated toroidal windings and PM or DC wave winding excitation," in *2023 IEEE Energy Conversion Congress and Exposition (ECCE)*, 2023, pp. 3845–3850.

[13] O. A. Badewa and D. M. Ionel, "Comparative analysis of motors with inner and outer reluctance rotors and PM stators," in *2024 IEEE Transportation Electrification Conference and Expo (ITEC)*, 2024, pp. 1–6.

[14] C. D. Manolopoulos, M. F. Iacchetti, A. C. Smith, P. Miller, and M. Husband, "Litz wire loss performance and optimization for cryogenic windings," *IET Electric Power Applications*, vol. 17, no. 4, pp. 487–498, 2023.

[15] J. He, Q. Yang, and Z. Wang, "On-line fault diagnosis and fault-tolerant operation of modular multilevel converters — a comprehensive review," *CES Transactions on Electrical Machines and Systems*, vol. 4, no. 4, pp. 360–372, 2020.

[16] D. D. Lewis, O. A. Badewa, A. Mohammadi, M. Vatani, and D. M. Ionel, "Fault tolerant electric machine concept for aircraft propulsion with PM rotor and DC current stator dual-stage excitation," in *2023 12th International Conference on Renewable Energy Research and Applications (ICRERA)*, 2023, pp. 607–611.

[17] S. Zhang, O. Wallscheid, and M. Porrmann, "Machine learning for the control and monitoring of electric machine drives: Advances and trends," *IEEE Open Journal of Industry Applications*, vol. 4, pp. 188–214, 2023.

[18] M. Omar, M. Bakr, and A. Emadi, "Switched reluctance motor design optimization: A framework for effective machine learning algorithm selection and evaluation," in *2024 IEEE Transportation Electrification Conference and Expo (ITEC)*, 2024, pp. 1–6.

[19] *Ansys® Electronics, version 24.1, 2024, ANSYS Inc.*

[20] Y. Liao, F. Liang, and T. Lipo, "A novel permanent magnet motor with doubly salient structure," *IEEE Transactions on Industry Applications*, vol. 31, no. 5, pp. 1069–1078, 1995.

[21] O. A. Badewa, A. Mohammadi, D. D. Lewis, D. M. Ionel, S. Essakiappan, and M. Manjrekar, "Optimization of an electric vehicle traction motor with a PM flux intensifying stator and a reluctance outer rotor," in *2023 IEEE Transportation Electrification Conference & Expo (ITEC)*, 2023, pp. 1–6.

[22] M. Lehr, D. Dietz, and A. Binder, "Electromagnetic design of a permanent magnet flux-switching-machine as a direct-driven 3 MW wind power generator," in *2018 IEEE International Conference on Industrial Technology (ICIT)*, 2018, pp. 383–388.

[23] V. Rallabandi, B. Ozpineci, and P. Kumar, "How EVs can escape the rare earth trap: Promising experimental motors are using exotic materials and ingenious configurations," *IEEE Spectrum*, vol. 61, no. 8, pp. 36–41, 2024.

[24] N. Taran, D. M. Ionel, V. Rallabandi, G. Heins, and D. Patterson, "An overview of methods and a new three-dimensional FEA and analytical hybrid technique for calculating AC winding losses in PM machines," *IEEE Transactions on Industry Applications*, vol. 57, no. 1, pp. 352–362, 2021.

[25] G. Volpe, M. Popescu, F. Marignetti, and J. Goss, "AC winding losses in automotive traction e-machines: A new hybrid calculation method," in *2019 IEEE International Electric Machines Drives Conference (IEMDC)*, 2019, pp. 2115–2119.

[26] M. Popescu and D. G. Dorrell, "Proximity losses in the windings of high speed brushless permanent magnet AC motors with single tooth windings and parallel paths," *IEEE Transactions on Magnetics*, vol. 49, no. 7, pp. 3913–3916, 2013.

[27] S. Lee, W. Lee, M. Liu, and B. Sarlioglu, "High-frequency motor impedance analysis and CM current estimation of electric motors with concentrated and toroidal windings," *IEEE Transactions on Transportation Electrification*, pp. 1–1, 2024.

[28] J. A. Swanke and T. M. Jahns, "Reliability analysis of a fault-tolerant integrated modular motor drive for an urban air mobility aircraft using Markov chains," *IEEE Transactions on Transportation Electrification*, vol. 8, no. 4, pp. 4523–4533, 2022.